Dynamics of Water-Soluble Stilbene Dendrimers upon Photoisomerization

Hiroshi Tatewaki,[†] Naoki Baden,[†] Atsuya Momotake,[‡] Tatsuo Arai,[‡] and Masahide Terazima*[,†]

Department of Chemistry, Graduate School of Science, Kyoto University, Kyoto 606-8502, Japan, and Department of Chemistry, University of Tsukuba, Tsukuba, Ibaraki 305-8571, Japan

Received: April 7, 2004; In Final Form: June 9, 2004

The energy-releasing process and the conformational dynamics of water-soluble stilbene dendrimers upon photoexcitation are studied by the time-resolved transient grating method. While the energy relaxation and the conformational change are completed within 30 ns for the first generation (W-G1), slower dynamics are observed for the second (W-G2) and the third (W-G3) generations. The enthalpy change by the photoisomerization increases and the dynamics of the conformational change becomes slower with an increase in the generation. The diffusion coefficients (*D*) of the trans- and cis-forms of W-G2 and W-G3 are almost the same, whereas a slight difference is observed for W-G1. These characteristic features are consistently explained in terms of the electric charges on the dendron surface.

1. Introduction

In many photoreactive biological proteins, such as the rhodopsin family or photoactive yellow protein (PYP), the photon energy is used to activate the protein conformation. This activation is triggered by a photoisomerization of a C═C double bond.[1−4] A chromophore with a C═C bond is generally bound to a large protein part, and the strain caused by the trans−cis isomerization leads to the subsequent conformational change of the protein. The isomerization reaction mechanism, the conformational dynamics, as well as the energetic relaxation of polyenes connected with large and massive environments have been attracting many scientists in various fields, because they could be suitable models for the photoactive biological proteins. For example, to explain the efficient isomerization reaction with a bulky group such as the retinal isomerization in rhodopsins, several isomerization mechanisms of the C═C double bond have been proposed.[5−8]

One such model connected with a large environment is a dendrimer with a photoisomerizable core. Dendrimers are supramolecules possessing well-defined repeating branches and a central core.[9−17] Recently, dendrimers of the stilbene core with a benzyl ether-type dendron (stilbene dendrimer: SD) have been synthesized, and the photochemical properties have been investigated.[18−21] The stilbene with the bulky dendrons isomerizes within a lifetime of ∼10 ns regardless of the size of the dendron. Although such isomerization by the C═C double bond twisting is expected to need a large volume change, the fluorescence lifetimes were reported not to depend on the solution viscosity,[20] which suggests that the photoisomerization of the stilbene dendrimers proceeds by a volume conserving mechanism rather than conventional 180° rotation around the C═C double bond.[18−20] Previously, we have investigated the energy-releasing process and the volume change upon the photoexcitation of the zeroth (G0), the first (G1), the second (G2), and the fourth (G4) generations of the stilbene dendrimers (SD) in time-domain by the transient grating (TG) technique.[21] We found a slow thermal energy release with about 50 ns lifetime for G0−G2, and this dynamics was attributed to the relaxation from the lowest excited triplet (T_1) state to the ground state. The conformational change of the dendron part of these generations should be faster than this lifetime (50 ns). On the other hand, a slightly slower dynamics was observed for G4 with a lifetime of ∼80 ns, which may be attributed to the conformational change of the dendron part after the trans−cis isomerization of the stilbene core. The volume change was rather small as compared with the molecular volume. We also concluded that an internal energy storage due to the steric hindrance of the bulky dendron group is not large.

Considering the analogy with biological proteins, it would be desirable that the model system is soluble in aqueous solution. Here, we investigate the first (W-G1), the second (W-G2), and the third (W-G3) generations of water-soluble stilbene dendrimers (WSD) (Figure 1)[22−24] by the TG method. The outer part of the dendron of these WSDs possesses many charged groups. The photochemical properties and the molecular dynamics of these dendrimers could be different from those of the neutral dendrimers (SD), because of these surface charges. It is also possible that the energy storage due to the congested dendron or the intermolecular interaction is significantly altered. We studied the conformational change and the diffusion process of WSDs after the photoisomerization of the stilbene core by the TG technique. Several interesting generation-dependent dynamics were observed. The photophysical dynamics of W-G1 after the photoisomerization is rather simple; the excess energy is released as heat within 30 ns, and, after that, only the molecular diffusion process takes place. On the other hand, W-G3 exhibits additional slow dynamics in two time regions: submicrosecond and millisecond. We attribute these dynamics to the slow conformational changes of the dendron part. The molecular energy of the cis-form is relatively higher than that of the trans-form. These kinetic and energetic properties are consistently explained in terms of the surface charges of W-G3.

2. Methods and Experimental Section

The TG technique is a detection method of the spatial modulation of the refractive index change that is induced by

* Corresponding author. Telephone: +81-75-753-4026. Fax: +81-75-753-4000. E-mail: mterazima@kuchem.kyoto-u.ac.jp.
[†] Kyoto University.
[‡] University of Tsukuba.

10.1021/jp048474y CCC: $27.50
Published on Web 07/16/2004

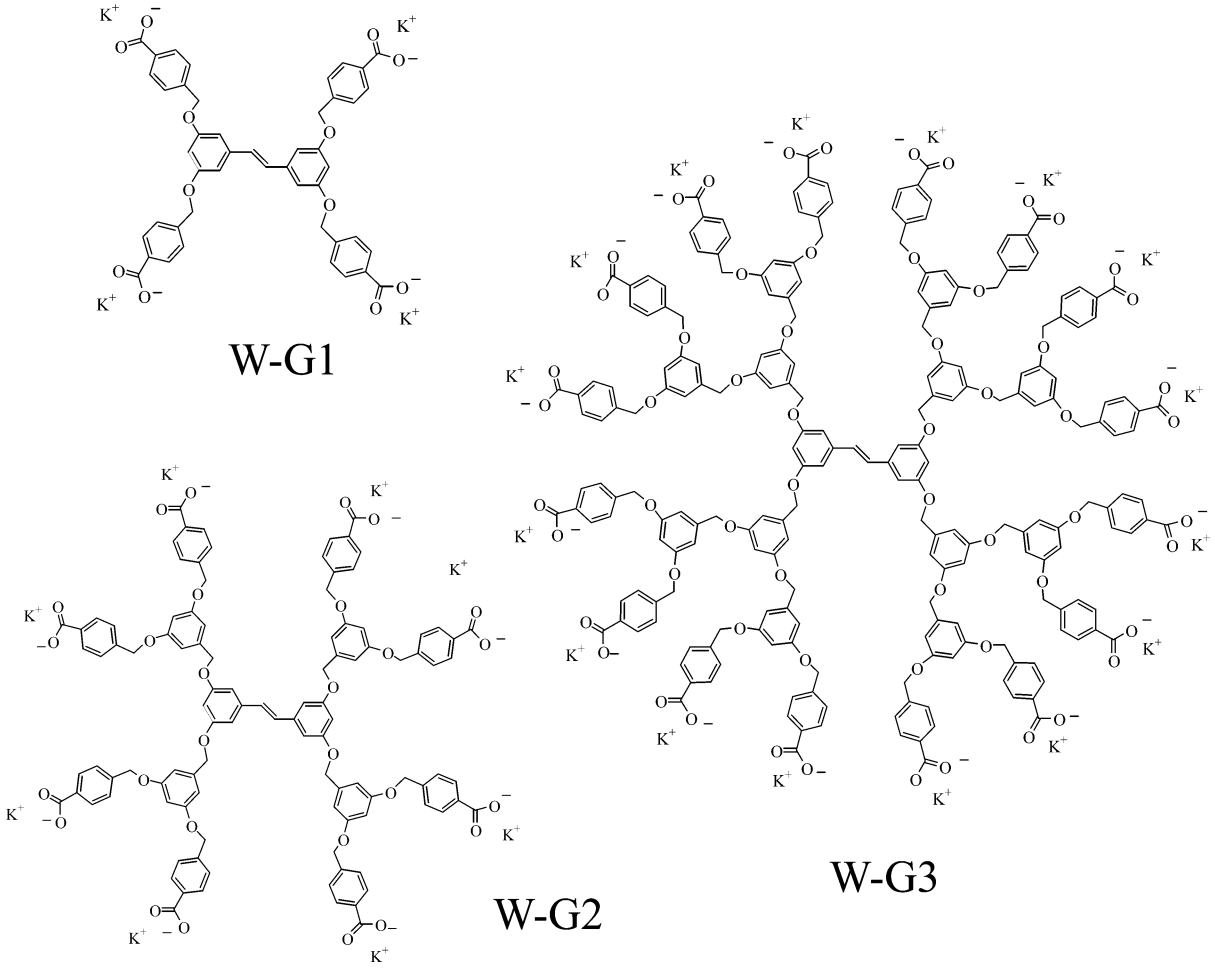

Figure 1. Molecular structures of the studied water-soluble stilbene dendrimers.

the interference light pattern between two light waves in time-domain.[25−29] The refractive index change mainly comes from the thermal energy release (thermal grating) and created (or depleted) chemical species by the photoreaction (species grating). In the species grating, there are two contributions: the population grating term due to the absorption spectrum change and the volume grating term due to the molecular volume change.[29] Using these components, we can study the volume change and energy change associated with chemical reactions in time-domain. The TG intensity under the present experimental conditions is proportional to the sum of the squares of the refractive index (δn; phase grating) and the absorbance changes. Because absorption of the trans- and cis-forms of WSDs is negligible at the probe wavelength (633 nm), the TG signal comes from the refractive index change upon the photoexcitation. The TG signal intensity (I_{TG}) can be simply represented as follows.

$$I_{TG}(t) = \alpha(\delta n_{th}(t) + \delta n_p(t) - \delta n_r(t))^2 \qquad (1)$$

where α is a constant, δn_{th}, δn_p, and δn_r are the refractive index changes of the thermal grating, that of the product, and that of the reactant, respectively. The minus sign for the term of δn_r reflects the depletion of the reactant by photoirradiation.

The experimental setup for the TG experiment was similar to that reported previously.[30−32] Briefly, a beam of an excimar laser (308 nm, XeCl) was split into two beams and crossed again at the sample cell to make the optical interference pattern. A He−Ne laser beam (633 nm) was used as a probe beam. The diffracted probe beam (TG signal) was isolated from the excitation laser light with a glass filter (Toshiba R-60) and a pinhole. The signal was detected by a photomultiplier tube (Hamamatsu R-928) and fed into a digital oscilloscope (Tetronix TDS-520). The TG signal was averaged by a microcomputer to improve the signal-to-noise (S/N) ratio.

The dendrimers were synthesized and purified as reported previously.[22−24] The WSDs were dissolved in alkali aqueous solutions (KOH solution: 4.1 mM for W-G1, 70 mM for W-G2, and 16 mM for W-G3). The laser power for the excitation of the sample was adjusted below 2 μJ/pulse. The sample solutions were prepared just before the measurement in a dark room. The solution was changed to a fresh one after every 200 shots of the excitation laser pulses. The repetition rate of the excitation laser was less than 1 Hz. The size of the excitation beam at the sample position was ca. 1 mm ϕ. The irradiated volume is small (typically ca. 4×10^{-3} cm^3) as compared with the entire volume of the sample solution, 0.5 mL. All measurements were carried out at 21 °C. The value of the grating wavenumber q was determined from the decay rate of the thermal grating signal of a calorimeter reference sample, bromocresol purple (BCP), which gives rise to only the thermal grating signal due to the nonradiative transition within the pulse width of the excitation laser.[30−32]

3. Results and Discussion

3.1. Photoisomerization Reaction and Enthalpy Change. The TG signal of the calorimetric reference sample (BCP), which releases the energy of the excited state quickly, is depicted in Figure 2a and b on different time scales. The calorimetric

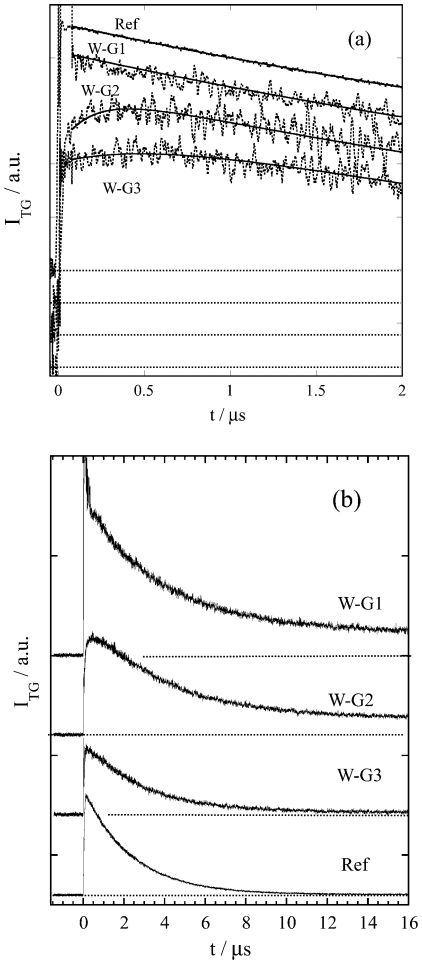

Figure 2. Observed TG signals after photoexcitation of the calorimetric reference sample, W-G1, W-G2, and W-G3, in alkali aqueous solution under the air-saturated solution (a) in a submicrosecond and (b) in 10 μs time regions (dotted curves) at $q^2 = 1.47 \times 10^{12}$ m^{-2}. The signals are shifted vertically to avoid the overlap. The broken lines denote the baselines for these signals. The samples are indicated in the figure. 'Ref' denotes the calorimetric reference sample. In (a), the best-fitted curves with eq 5 are shown by the solid lines.

reference signal rises with a time response of our system (ca. 20 ns) and decays to the baseline completely with the rate constant of $D_{th}q^2$ (D_{th}, the thermal diffusivity of the solution; q, the grating wavenumber). This characteristic decay rate constant is a clear indication that the origin of the signal is the thermal grating. The temporal profile of the thermal grating is given by[28,29]

$$\delta n_{th}(t) = \delta n_{th}{}^{0} \exp(-D_{th}q^2 t) \qquad (2)$$

The TG signals of W-G1, W-G2, and W-G3 in alkali aqueous solution under the air-saturated solution are also depicted in Figure 2 within a few microseconds time region after the photoexcitation. The absorbance of the sample at the excitation wavelength is adjusted to be the same as that of the calorimetric reference solution so that the intensities of these signals can be compared quantitatively.

The signals for all samples rise with the time response of our system. After this rise, the TG signal of W-G1 shows rapid decay. We have confirmed that this spike-like signal in this time range is not due to fluorescence or light scattering of the excitation pulse, but it is the TG signal. Because the decay rate of this fast response signal is slower than the pulse width of the excitation light, this is not a coherent spike. The origin of this signal of W-G1 must be attributed to the population grating due to the excited singlet (S_1) state, of which the lifetime is about 15 ns (Table 1). In this paper, we will focus our attention on the conformational change of the dendron part after the isomerization of the central part; we are not going to consider this fast decaying signal.

TABLE 1: Properties of Water-Soluble Stilbene Dendrimers (W-G1, W-G2, and W-G3) in Alkali Aqueous Solution[a]

solute	W-G1	W-G2	W-G3
Φ_f	0.21	0.05	0.17
τ_f/ns	15	11/2.1	11/3.7
E_f/kJ mol^{-1}	279	287	303
Φ	0.17	0.47	0.15
τ_s/ns		180	800
$\delta n^s/\delta n_{th}^{ref}$		0.17	0.27
$\Phi\Delta H$/kJ mol^{-1}	30 ± 10	100 ± 10	46 ± 10
ΔH/kJ mol^{-1}	170 ± 60	210 ± 20	308 ± 60
$D_t/10^{-10}$ m^2/s	2.8	1.5	0.97
$D_c/10^{-10}$ m^2/s	3.5	1.5	0.97
r/nm	0.58	0.76	0.97
$D_{SE}/10^{-10}$ m^2/s	3.7	2.8	2.2

[a] Φ_f, fluorescence quantum yield;[24] τ_f, fluorescence lifetime;[24] E_f, average photon energy of the fluorescence; Φ, reaction quantum yield;[24] τ_s, lifetime of the slow rise component; $\delta n^s/\delta n_{th}^{ref}$, amplitude of the slow rising component normalized by the refractive index change of the calorimetric reference sample; ΔH, enthalpy change for the trans-to-cis isomerization reaction; D_t, diffusion coefficients of the trans-form; D_c, diffusion coefficients of the cis-form; r, calculated molecular radius by the atom increment method; D_{SE}, calculated D based on the Stokes−Einstein relationship. The fluorescence of W-G2 and W-G3 decays biexponentially, and the two lifetimes are listed.[24]

The population grating signal due to the S_1 state is weak for W-G2 and W-G3. After the rapid rising, the TG signals of W-G2 and W-G3 show additional weak slower rising components (Figure 2a). All of the signals decay to constant intensities in the microsecond time region (Figure 2b). Because this decay rate constant agrees well with $D_{th}q^2$, the main part of the signal in this time range is due to the thermal grating signal, which is produced by the thermal energy coming from the nonradiative transition and the enthalpy change of the reaction. The constant signals at around 10 μs represent the species grating signal, which reflects the absorbance change and the volume change associated with the isomerization reaction. We will describe and analyze the temporal profile of this component in the next section.

The thermal grating signal intensity represents the released energy from the molecule. First, we investigate the enthalpy change (ΔH) of the isomerization reaction from the thermal grating signal intensity. The magnitude of $\delta n_{th}{}^{0}$ is expressed by

$$\delta n_{th}{}^{0} = \frac{dn}{dT}\frac{h\nu\phi W}{\rho C_P}\Delta N \qquad (3)$$

where dn/dT is the temperature dependence of the refractive index, $h\nu$ is the photon energy of the excitation light (389 kJ/mol), ρ is the density, C_p is the heat capacity at a constant pressure, and W is the molecular weight. Furthermore, ϕ is the quantum yield of the nonradiative transition and is given by

$$\phi = (h\nu - \Phi\Delta H - \Phi_f E_f)/h\nu \qquad (4)$$

where ΔH is defined by the enthalpy change from the reactant to the product, Φ is the quantum yield of the chemical reaction,

Φ_f is the quantum yield of fluorescence, and E_f is the average photon energy of the fluorescence.

For determining the enthalpy difference between the trans- and cis-forms (ΔH), we quantitatively measured δn_{th}^0 under a weak laser power region, in which the species grating signal intensity is linear to the square of the excitation laser power. Using the TG technique, the thermal contribution can be separated from the other contributions by signal fitting with the characteristic time constant of the thermal diffusion ($D_{th}q^2$) so that there is no disturbance from the other contributions of the TG signal.[29−33] For eliminating the unknown constant α in eq 1 and other quantities in eq 3 (dn/dT, ΔN, etc.), the thermal grating signal intensity of the sample is divided by that of the calorimetric reference. From these ratios and reported fluorescence quantum yields, $\Phi\Delta H$ values are determined as 30 ± 10, 100 ± 10, and 46 ± 10 kJ/mol for W-G1, W-G2, and W-G3, respectively. The larger value of $\Phi\Delta H$ for W-G2 reflects the larger quantum yield of the reaction (Φ) (Table 1).

One of the interesting subjects of the photophysical properties of dendrimers is the energy flow process from the dendron. Previously, it was proposed that a significant amount of energy of the excitation photon could be stored in the dendron part for some dendrimers.[16,17] However, we have shown that the energy storage for SDs is not large by using the thermal grating intensity.[21] For these WSDs, because the reaction quantum yield (Φ) is relatively small in particular for W-G1 and W-G3, the absolute value of ΔH is sensitive to the accuracy of these reported Φ values. Hence, it is difficult to discuss the absolute values. However, we should note that the $\Phi\Delta H$ values of WSDs (30−100 kJ/mol) are larger than those of SDs (21−24 kJ/mol) measured before.[21] These large values imply that the cis-forms of WSDs are more destabilized than those of SDs. Because the only difference between WSD and SD is the charges on the dendron surface of WSD, it may be reasonable to consider that this destabilization of the cis-form comes from the effect of these electric charges. As compared with the rather uniform charge distribution on the surface of the trans-form, the charge distribution of the cis-form is expected to be nonuniform based on the molecular conformation (e.g., Figure 4 in ref 21). Hence, the electrostatic repulsion between the charges should be larger for the cis-form than that for the trans-form. This electrostatic repulsion may be the cause of the larger ΔH. It is particularly interesting to note that ΔH becomes larger with an increase in the generations. This generation dependence may reflect the crowding of the electric charges, which is consistent with the above interpretation.

3.2. Conformational Change after Isomerization. Because the dendron part is connected to the central stilbene moiety by the chemical bond, the stable configuration of the dendron side chain should be significantly different between the trans- and cis-forms of the stilbene. Even when the stilbene moiety is photoisomerized rapidly, the large side chain may not respond suddenly. This time-delay should be the cause of the slower thermal reaction of some photoreactive proteins despite the very fast triggering (isomerization) reactions.[1−4] It is interesting to see how fast the large moiety moves to adjust to the new configuration. However, such side-chain dynamics is difficult to detect by the traditional flash photolysis technique, because most of the side-chain changes are spectrally silent. Recently, it has been shown that the conformational change of proteins can be detected sensitively as the molecular volume change.[30−33] We investigated the volume change of WSDs in time-domain to observe the dynamics of the dendrons.

Any dynamics that can be attributed to the conformational change is not observed for W-G1 in the whole time range. On the other hand, the conformational change in the submicrosecond time region is observed as the slow rising component of the thermal grating signal for W-G2 and W-G3 (Figure 2a). The rise portion in the submicrosecond time range is fitted well by a function of

$$\delta n(t) = \delta n^{tot} - \delta n^{s} \exp(-t/\tau_s) \quad (5)$$

where δn^{tot} and δn^{s} are the total refractive index change and the slow component, respectively, and τ_s is the lifetime of the slow rising component. The lifetimes of these components are 180 ns for W-G2 and 800 ns for W-G3 (Table 1).

Previously, we have found a similar slow rising component in the submicrosecond region after photoexcitation of G0, G1, G2, and G4 of SD in THF.[21] The dynamics for G0, G1, and G2 with a lifetime of ~50 ns has been attributed to the relaxation from the excited triplet (T_1) state of the stilbene core. However, on the contrary, we do not believe that the slow dynamics for W-G2 and W-G3 represents the relaxation of the T_1 state, because of the following reasons. First, the slow rising component is observed only for W-G2 and W-G3, not W-G1. Although it might be possible that the congestion of the dendron part changes the photophysical properties such as the S_1-T_1 intersystem crossing yield, the fact that all generations of SD exhibit similar slow dynamics may exclude this possibility. It is unlikely that the intersystem crossing to the T_1 state is effective only for the larger generations. Second, even when the solution is saturated with oxygen molecules (O_2), the slow dynamics does not change. Because the T_1 state should be quenched efficiently by O_2, this is good evidence against the T_1 state relaxation. Again, the congested side chain may change the oxygen effect to the T_1 state. However, we have found that the oxygen effect does not change from G1 to G4 for SD previously.[21] This fact means that the dendron part of even G4 is not so congested to prevent the entering oxygen molecule from the central part. Therefore, we attributed this rising component to the slow conformational change of the dendron part after the photoisomerization of this stilbene core. The fact that the observed lifetime of this component becomes longer with an increase in the size of the dendron parts (no dynamics slower than 50 ns for W-G1, 180 ns for W-G2 and 800 ns for W-G3) may support this assignment.

Previously, the 80 ns dynamics observed for G4 of SD was attributed to the conformational change of the dendron part.[21] It is interesting to note that the lifetime of the slow component for W-G3 is much slower than that of G4, although the size of the dendron is much larger for G4. This difference may originate from the surface charge of W-G3. As was stated in previous section, the electrostatic repulsion between the negative charges on the surface is expected to be larger for the cis-form than that of the trans-form. This electrostatic repulsion can slow the conformational dynamic after the isomerization of the stilbene core.

Another conformational change is observed in the species grating signal on a much longer time scale. The signals of the dendrimers after the completely decay of the thermal grating signal correspond to the difference in the species grating signals between the trans- and cis-forms (eq 1). The TG signals in a longer time region were depicted in Figure 3. Considering the observation time range and the negligible slow thermal back reaction from the cis- to the trans-form, one may attribute the dynamics to the molecular diffusion process and the structural

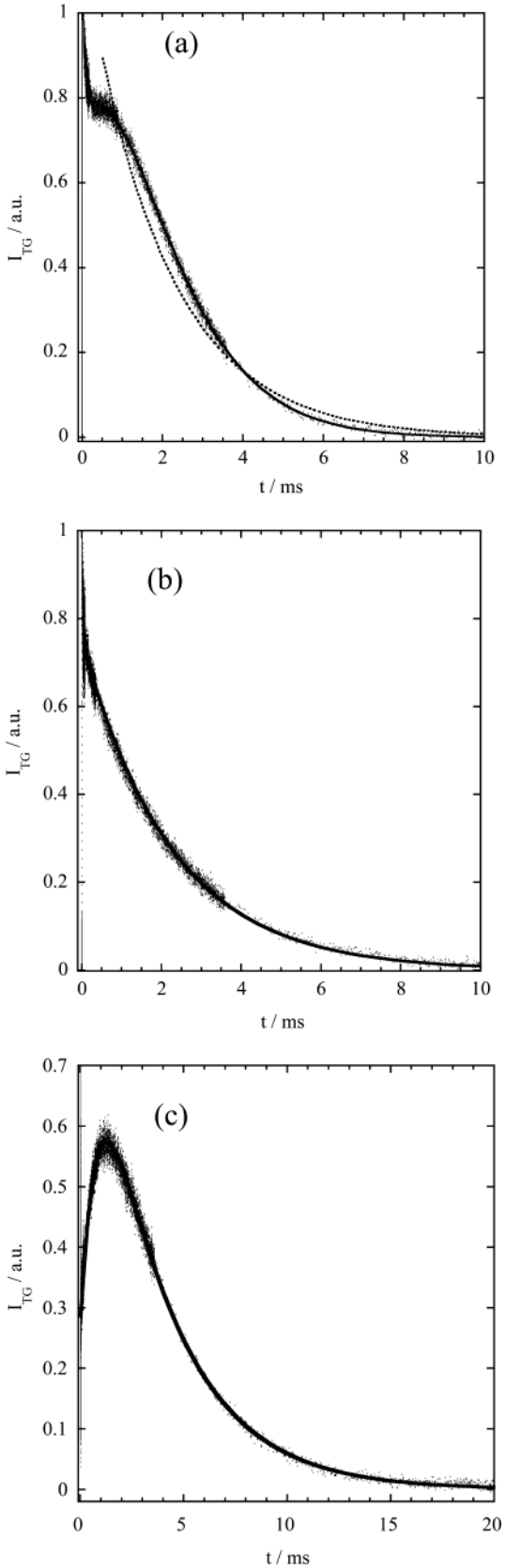

Figure 3. TG signals (dotted lines) of (a) W-G1, (b) W-G2, and (c) W-G3 in alkali aqueous solution under the air-saturated solution in a millisecond time region. The solid lines indicate the best-fitted curves by eqs 1, 6, and 7. The broken line in (a) is an example of the fitted curve by the single-exponential function to show that the fitting is not good.

change. Both dynamics can be distinguished by examining the q^2-dependence of the rate constant.

For instance, if the structural change in the observing time range is negligible, the temporal profile of the species grating signal is expressed by a molecular diffusion equation and is given by[29−33]

$$\delta n_{spe}(t) = \delta n_{spe}{}^{0} \exp(-Dq^2 t) \quad (6)$$

where D is the molecular translational diffusion coefficient. If the D values of the trans- and the cis-forms are different, the observed species grating signal should be expressed by a biexponential function.

$$\delta n_{spe}(t) = -\delta n_t \exp(-D_t q^2 t) + \delta n_c \exp(-D_c q^2 t) \quad (7)$$

where D_t and D_c are the diffusion coefficients of the trans- and cis-forms, respectively. The preexponential factors, δn_t and δn_c, are refractive index changes due to the presence of the trans- and the cis-forms, respectively. Because the trans-form is depleted by photoexcitation, the signs of δn_t and δn_c should be negative and positive, respectively (eq 1). The q^2-dependent dynamics is a clear indication of the diffusion process. On the other hand, the dynamics of the structural change should not depend on q^2.

The relatively strong species grating signal is observed for W-G2 and is depicted in Figure 3b. It is well fitted by a single-exponential function. This rate is proportional to q^2 as shown in Figure 4b, which indicates that the decay of the signal is determined by the diffusion process. The single-exponential decay means that the D values of the trans- and cis-forms are very close each other (i.e., $D_t = D_c = 1.5 \times 10^{-10}$ m^2/s in eq 7) and there is no observable conformational dynamics in this time range.

On the contrary to this rather simple species grating signal of W-G2, those of W-G1 and W-G3 cannot be reproduced by a single-exponential function. The species grating signal of W-G1 decreases monotonically, but a calculated curve with a single exponential function deviates from the observed signal significantly (Figure 3a). The signal can be reproduced by a biexponential function almost perfectly. Plotting the rate constants against q^2, we found that both rate constants linearly depend on q^2 (Figure 4b). This linear dependence shows that there are two diffusing species with different rates (eq 7). Considering the sign of the refractive index change based on a fact that there is no interference dip between the thermal grating and the species grating signals, we found $D_c > D_t$, and, from the q^2 plot, we obtained $D_c = 3.5 \times 10^{-10}$ m^2/s, and $D_t = 2.8 \times 10^{-10}$ m^2/s. It is worthy of note that there is no conformational (i.e., q-independent) dynamics in this time range for W-G1, as well.

The species grating signal of W-G3 can be also fitted by a biexponential function. However, contrary to W-G1, while one of the rate constants depends on q^2, the other does not (Figure 4c). From the q^2-dependent rate constant, $D_c = D_t$ is determined to be 0.97×10^{-10} m^2/s. As stated above, the q^2-independent rate constant (∼1 ms) represents the molecular dynamics except the diffusion process. Considering that the trans−cis isomerization completes within 15 ns as reported from the fluorescence lifetime measurement,[24] we may attribute this dynamics to the conformation change of the dendron part.

In the previous section, we showed the conformational dynamics with the 800 ns time constant. Therefore, we observe two conformational dynamics in different time regions, 800 ns and 1 ms. It would be interesting to note that the time-scales of these dynamics are about 1000 times different. In sequential

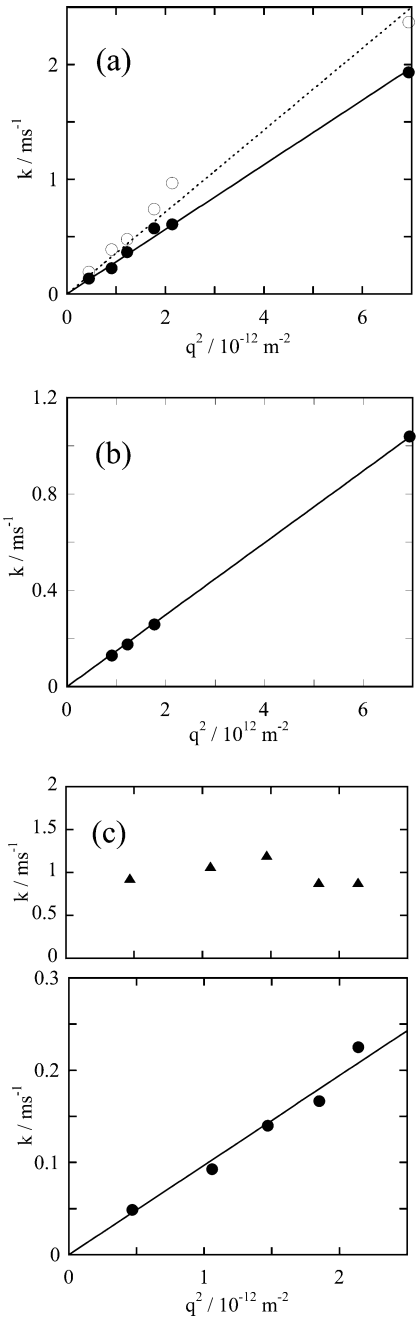

Figure 4. The q^2 plot of the decay rate constants (k) of the species grating signals of (a) W-G1, (b) W-G2, and (c) W-G3. In (a), the open circles and closed circles denote cis- and trans-isomers, respectively. The linear lines represent the best-fitted ones by $k = Dq^2$. The slopes of the plots represent the diffusion coefficients.

reaction schemes of some photosensitive proteins, it has been frequently reported that the lifetimes of the protein conformation changes differ by about 3 orders of magnitude.[1−2,30] We do not have a clear answer as to why there are two dynamics with such largely different lifetimes at present. We may speculate that the faster one represents the rearrangement of the mobile part of the dendron and the slower one is due to the final adjustment of the other portion to the new conformation. The details of the dynamics should be investigated in the future. This dendrimer system will be a good model for the study of the conformation change by a bulky group triggered by the photoisomerization reaction.

3.3. Molecular Diffusion. Frequently, a diffusion coefficient of a molecule in liquid solution has been compared with a theoretically calculated one on the basis of the Stoke−Einstein equation,[34]

$$D_{SE} = k_B T/6\pi\eta r \tag{8}$$

where k_B is the Boltzmann constant, T is the temperature, η is the viscosity, and r is the radius of a spherical molecule. The calculated D values using this equation are listed in Table 1. The radii of the dendrimers were calculated from the van der Waals volume obtained from the atomic increment method.[35] We should note that the observed D is much smaller than the calculated D. The smaller D than predicted from eq 8 is explained in terms of the strong solute−solvent interaction. The electric charge on the side chain enhances the intermolecular interaction, which results in the larger friction and, hence, smaller D.

Not only the small magnitude of D, but also two other diffusion properties should be noted. First, according to eq 8 and the calculated molecular radii (Table 1), the ratio of D of W-G3 to D of W-G2 should be 0.78. However, the observed ratio (0.65) is much smaller. This smaller ratio than expected should reflect the larger number of charges for W-G3 than for W-G2. Hence, D of W-G3 is much smaller than that expected from the molecular radius.

Second, because the van der Waals volume does not depend on the conformation of the dendrimers, the Stoke−Einstein equation predicts that D_t should be the same as D_c. This prediction agrees with the observation for W-G2 and W-G3. On the contrary, D_t is smaller than D_c for W-G1. Previously, we found that D_t is almost the same as D_c for the smaller dendrimers, but the difference becomes larger with the generations ($D_t > D_c$).[21] In this case, the generation-dependent difference between D_t and D_c was explained in terms of the surface roughness of the dendron part. The opposite behavior of WSD as compared with SD may be rationalized by considering that the dominant part of the friction for the translational diffusion is determined by the electric charges and not by the geometric conformation of the dendron; that is, the difference in D due to the different conformation is overcome by the friction due to the electric change, which should be conformation-independent. Hence, the larger generations (W-G2 and W-G3), which possess larger frictions due to the electric interaction, have similar D values between the trans- and cis-forms.

4. Conclusion

The enthalpy change and the conformational dynamics of the first, second, and third generations of water-soluble stilbene dendrimers are studied by the pulsed laser induced transient grating technique in time-domain. For W-G1, the energy relaxation as well as the conformational change complete within 30 ns. However, a slower dynamics of ∼180 ns is observed for W-G2. The conformational dynamics of W-G3 is found to be further slower (∼800 ns and ∼1 ms). These dynamics are attributed to the conformational change of the dendron part to adjust to a new position for the cis-form. The enthalpy of the cis-form is much larger than that of the trans-form. The diffusion coefficients of the WSDs are smaller than those calculated by the Stoke−Einstein relationship. These characteristic features can be explained in terms of the electric charges on the dendron surface.

Acknowledgment. This work was supported by a Scientific Research Grant-in-Aid (No. 13853002) and that for the Priority Area (417 and 430/No. 15076204) from the Ministry of Education, Science, Sports, and Culture of Japan.

References and Notes

(1) Schoenlein, R. W.; Peteanu, L. A.; Mathies, R. A.; Shank, C. V. *Science* **1991**, *254*, 412. Oesterhelt, D.; Stoeckenius, W. *Proc. Natl. Acad. Sci. U.S.A.* **1973**, *70*, 2583. Oesterhelt, D.; Tittor, J. *Trends Biochem. Sci.* **1989**, *14*, 57.

(2) Dartnall, H. J. A. *Handbook of Sensory Physiology, Photochemistry of vision photosensitivity*; Springer-Verlag: New York, 1972. Mathies, R. A.; Lin, S. W.; Ames, J. B.; Pollard, E. T. *Annu. Rev. Biophys. Biophys. Chem.* **1991**, *20*, 491.

(3) Baca, M.; Borgstahl, G. E. O.; Boissinot, M.; Burke, P. M.; Williams, D. R.; Slater, K. A.; Getzoff, E. D. *Biochemistry* **1994**, *33*, 14369.

(4) Hoff, W. D.; Düx, P.; Hård, K.; Devreese, B.; Nugteren-Roodzant, I. M.; Crielaard, W.; Boelens, R.; Kaptein, R.; van Beeumen, J.; Hellingwerf, K. J. *Biochemistry* **1994**, *33*, 13959.

(5) Liu, R. S. H.; Asato, A. E. *Proc. Natl. Acad. Sci. U.S.A.* **1985**, *82*, 259.

(6) Liu, R. S. H.; Hammond, G. S. *Proc. Natl. Acad. Sci. U.S.A.* **2000**, *97*, 11153.

(7) Müller, A. M.; Lochbrunner, S.; Schmidt, W. E.; Füss, W. *Angew. Chem., Int. Ed.* **1998**, *37*, 505.

(8) Alfimov, M. V.; Razumov, V. F.; Rachinsky, A. G.; Listvan, V. N.; Scheck, Y. B. *Chem. Phys. Lett.* **1983**, 593.

(9) Ottaviani, M. F.; Andechaga, P.; Turro, N. J.; Tomalia, D. A. *J. Phys. Chem. B* **1997**, *101*, 6057. Ottaviani, M. F.; Matteini, P.; Brustolon, M.; Turro, N. J.; Jockusch, S.; Tomalia, D. A. *J. Phys. Chem. B* **1998**, *102*, 6029.

(10) Neuwahl, F. V. R.; Righini, R.; Adronov, A.; Malenfant, P. R. L.; Frechet, J. M. J. *J. Phys. Chem. B* **2001**, *105*, 1307. Swallen, S. F.; Zhu, Z.; Moore, J. S.; Kopelman, R. *J. Phys. Chem. B* **2000**, *104*, 3988. De Backer, S.; Prinzie, Y.; Verheijen, W.; Smet, M.; Desmedt, K.; Dehaen, W.; De Schryver, F. C. *J. Phys. Chem. A* **1998**, *102*, 5451.

(11) Fischer, M.; Vögtle, F. *Angew. Chem., Int. Ed.* **1999**, *38*, 884.

(12) Choi, M.; Aida, T.; Yamazaki, T.; Yamazaki, I. *Angew. Chem., Int. Ed.* **2001**, *40*, 74.

(13) Hearshaw, M. A.; Moss, J. R. *Chem. Commun.* **1999**, 1.

(14) Liao, L.-X.; Junge, D. M.; McGrath, D. V. *Macromolecules* **2002**, *35*, 319. Junge, D. M.; McGrath, D. V. *J. Am. Chem. Soc.* **1999**, *121*, 4912. Junge, D. M.; McGrath, D. V. *Chem. Commun.* **1997**, 857. Sheng, L.; McGrath, D. V. *J. Am. Chem. Soc.* **2000**, *122*, 6795.

(15) Archut, A.; Vögtle, F.; DeCola, L.; Azzellini, G. C.; Balzani, V.; Bamanujam, P. S.; Berg, R. H. *Chem.-Eur. J.* **1998**, *4*, 699. Archut, A.; Azzellini, G. C.; Balzani, V.; DeCola, L.; Vögtle, F. *J. Am. Chem. Soc.* **1998**, *120*, 12187.

(16) Jiang, D.-L.; Aida, T. *Nature* **1997**, *388*, 454.

(17) Wakabayashi, Y.; Tokeshi, M.; Hibara, A.; Jiang, D.-L.; Aida, T.; Kitamori, T. *J. Phys. Chem. B* **2001**, *105*, 4441.

(18) Mizutani, T.; Ikegami, M.; Nagahata, R.; Arai, T. *Chem. Lett.* **2001**, 1014.

(19) Imai, M.; Arai, T. *Tetrahedron Lett.* **2002**, *43*, 5265.

(20) Uda, M.; Mizutani, T.; Hayakawa, J.; Momotake, A.; Ikegami, M.; Nagahata, R.; Arai, T. *Photochem. Photobiol.* **2002**, *76*, 596.

(21) Tatewaki, H.; Mizutani, T.; Hayakawa, J.; Arai, T.; Terazima, M. *J. Phys. Chem. A* **2003**, *107*, 6515.

(22) Hayakawa, J.; Momotake, A.; Nagahata, R.; Arai, T. *Chem. Lett.* **2003**, *32*, 1008−1009.

(23) Hayakawa, J.; Momotake, A.; Arai, T. *Chem. Commun.* **2003**, 94−95.

(24) Momotake, A.; Hayakawa, J.; Nagahata, R.; Arai, T. *Bull. Chem. Soc. Jpn.* **2004**, *77*, 1195.

(25) Eichler, H. J.; Gunter, P.; Pohl, D. W. *Laser Induced Dynamic Gratings*; Springer-Verlag: Berlin, 1986.

(26) Fayer, M. D. *Annu. Rev. Phys. Chem.* **1982**, *33*, 63.

(27) Miller, R. J. D. *Annu. Rev. Phys. Chem.* **1991**, *42*, 581.

(28) Terazima, M. In *Advances in Multiphoton Processes and Spectroscopy*; Lin, S. H., Villaeys, A. A., Fujimura, Y., Eds.; World Scientific: Singapore, 1996; Vol. 10.

(29) Terazima, M. *Adv. Photochem.* **1998**, *24*, 255.

(30) Takeshita, K.; Hirota, N.; Imamoto, Y.; Kataoka, M.; Tokunaga, F.; Terazima, M. *J. Am. Chem. Soc.* **2000**, *122*, 8524. Takeshita, K.; Imamoto, Y.; Kataoka, M.; Tokunaga, F.; Terazima, M. *Biochemistry* **2002**, *41*, 3037. Takeshita, K.; Imamoto, Y.; Kataoka, M.; Mihara, K.; Tokunaga, F.; Terazima, M. *Biophys. J.* **2002**, *83*, 1567.

(31) Sakakura, M.; Yamaguchi, S.; Hirota, N.; Terazima, M. *J. Am. Chem. Soc.* **2001**, *123*, 4286. Sakakura, M.; Morishima, I.; Terazima, M. *J. Phys. Chem. B* **2001**, *105*, 10424. Sakakura, M.; Morishima, I.; Terazima, M. *Biochemistry* **2002**, *41*, 4837.

(32) Nishioku, Y.; Nakagawa, M.; Tsuda, M.; Terazima, M. *Biophys. J.* **2001**, *80*, 2922. Nishioku, Y.; Nakagawa, M.; Tsuda, M.; Terazima, M. *Biophys. J.* **2002**, *83*, 1136.

(33) Terazima, M. *J. Photochem. Photobiol., C* **2002**, *24*, 1−28.

(34) Cussler, E. L. *Diffusion*; Cambridge University Press: New York, 1984.

(35) Edward, J. T. *J. Chem. Educ.* **1970**, *47*, 261.